ISBN: 978-3-95450-184-7 doi:10.18429/JACoW-IPAC2018-THPML018

MODELING OF SELF-MODULATED LASER WAKEFIELD ACCELERATION DRIVEN BY SUB-TERAWATT LASER PULSES*

C.-Y. Hsieh, S.-H. Chen, Dept. of Physics, National Central Univ., Jhongli 32001, Taiwan
M.-W. Lin†, Inst. of Nucl. Engineering and Science, National Tsing Hua Univ., Hsinchu, Taiwan

Abstract

Laser wakefield accelerator (LWFA) can be achieved in a scheme in which a sub-terawatt (TW) laser pulse is introduced into a thin, high-density target [1]. As a result, the self-focusing and the self-modulation can greatly enhance the peak intensity of the laser pulse capable of exciting a nonlinear plasma wave to accelerate electrons. A particle-in-cell model was developed to study the sub-TW LWFA, in which a 0.6-TW laser pulse is injected into a hydrogen gas cell with a flat-top density profile. In addition to using 800-nm laser pulses, laser pulses of 1030 nm were used in simulations as they represent a viable approach to realize the sub-TW LWFA driven by high-frequency, diode-pumped laser systems [2]. Process of the electron injection is complicated in such a high-density plasma; however, the simulation results show that the appropriate injection and acceleration of electrons can be achieved by optimizing the length of the gas cell. When a 340-micrometer long gas cell is introduced, energetic electrons (> 1 MeV) are produced with a relatively low emittance of 3.5 π-mm-mrad and a total charge of 0.32 nC accordingly.

INTRODUCTION

A promising method for realizing a sub-TW LWFA is to operate LWFA at high plasma densities such that the initial laser peak power P_0 is higher than the self-focusing critical power [3]

$$P_{cr} = 17.4\frac{n_{cr}}{n_e}\ \mathrm{GW}, \qquad (1)$$

where the plasma critical density $n_{cr}=\epsilon_0 m_e\omega^2/q_e^2$ is determined by the vacuum permittivity ϵ_0, electron mass m_e, electron charge q_e, and laser frequency $\omega=2\pi c/\lambda$ (c is the vacuum speed of light) while n_e is the electron density. Subsequently, the induced self-focusing of the laser pulse can significantly increase the pulse intensity over the threshold of exciting nonlinear plasma waves. In addition to the self-focusing effect, the self-modulation instability grows up and shapes the laser pulse into a series of pulse train so that plasma bubbles can be excited by these longitudinally compressed micro pulses.

In this work, the interaction of sub-TW, 800-nm laser pulses with flat-top gas density profiles that can be produced in gas cells are defined and studied. Next, Laser pulses at 1030 nm are defined to study the scheme in which laser pulses produced from a high-repetition-rate, diode-pumped Ytterbium(Yb) laser system [4, 5] are applied to drive sub-TW LWFA.

* Work supported by the Ministry of Science and Technology in Taiwan.
† mwlin@mx.nthu.edu.tw

INTERACTION OF 800-nm LASER PULSES WITH FLAT-TOP DENSITY PROFILES

A 3-D PIC model has been developed using the commercial software package VORPAL [6]. The simulation framework is defined in the Cartesian coordinate system (x, y, z), in which a linearly polarized laser pulse propagates along the longitudinal x-axis. Figure 1(a) illustrates the transverse E_y field of a 50-fs (FWHM Gaussian pulse duration), 0.6-TW, 800-nm laser pulse that is focused to a FWHM diameter of w_D = 8.4 μm, which corresponds to the 40-mJ pulse introduced in Goers *et al.*s' experiments [1], while 80 % of the energy was enclosed in the laser spot. Figure 1(b) shows that the flat-top density profile of the gas target defined with a full length of 290 μm, including 40-μm density ramps existing at the front and back sides the simulations.

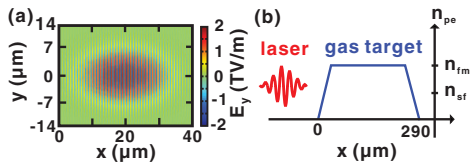

Figure 1: Snapshot of (a) transverse E_y electric field of a 50-fs, 0.6-TW, linearly polarized laser pulse with a diameter w_D = 8.4 μm; and (b) Illustration of the flat-top density profile along with the axial position x.

The interaction of a 800-nm laser pulse with a hydrogen gas target of a flat-top distribution having a peak density $n_{fm} = 10^{20} cm^{-3}$ in the plateau region is investigated first. This peak density gives the critical power P_{cr} = 0.3 TW and the ratio P_L/P_{cr} = 2. As shown in Figs. 2(a)-(b), the self-focusing and the self-modulation effects shape the laser pulse into four prominent micro pulses after a propagating distance of 220 μm. This modulation effect thus induces the longitudinal compression of the first micro pulse, which in turn excites a plasma bubble capable of inducing electron injection within it. As evidenced in Fig. 2(c), a significant amount of electrons having energies > 1 MeV appears at the edge of the first plasma bubble. The resulting energy spectra of the accelerated electron with a maximum energy about 20 MeV can be observed in Fig. 2(d).

When the density of the plateau region is reduced to n_{fm} = $5 \times 10^{19} \mathrm{cm}^{-3}$, the corresponding critical power of the self-focusing effect increases to P_{cr} = 0.6 TW. Under this condition, P_{cr} becomes equal to the peak power of the introduced 800-nm laser pulse and results shown in Fig. 3 indicate that corresponding plasma response cannot effectively drive the self-focusing of the laser pulse throughout its

ISBN: 978-3-95450-184-7 doi:10.18429/JACoW-IPAC2018-THPML018

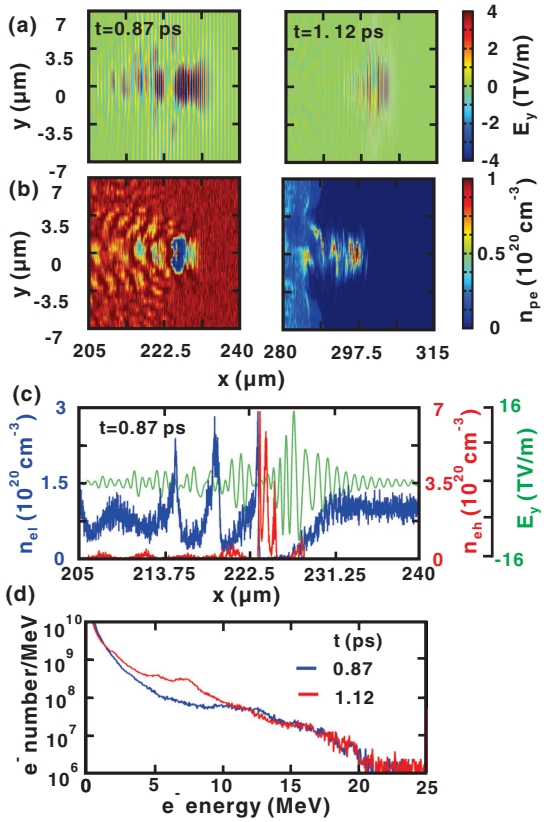

Figure 2: Variations of (a) the E_y field of the incident 800-nm laser pulse and (b) the density distribution of hydrogen plasma electrons. (c) Comparison of the on-axis densities of the accelerated electron n_{eh} (with energies > 1 MeV) and the plasma electrons n_{el} (with energies < 1 MeV). (d) Variations of the energy spectra about the electrons. The peak density $n_{fm} = 10^{20}\text{cm}^{-3}$ is assigned.

propagation in the target output. Therefore, it is understood that a sub-TW LWFA cannot be accomplished with such a low power ratio P_L/P_{cr} =1.

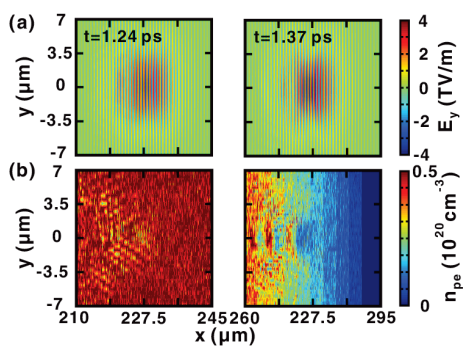

Figure 3: Variations of (a) the E_y field of the incident 800-nm laser pulse and (b) the density distribution of hydrogen plasma electrons. The peak density $n_{fm} = 5 \times 10^{19}\text{cm}^{-3}$ is assigned.

EFFECT OF USING 1030-nm LASER PULSES

Here, 1030-nm laser pulses with the same rest of parameters of the previously defined 800-nm laser pulses are assigned for investigations. As can be estimated by Eq. (1) about the critical power P_{cr}, the self-focusing of a laser pulse with a longer wavelength can be achieved when a lower gas/plasma density is applied.

By setting the density $n_{fm} = 5 \times 10^{19} cm^{-3}$ for the plateau region of a flat-top gas target, Fig. 4(a) illustrates the successfully achieved self-focusing of a 0.6-TW, 1030-nm laser pulse that can drive the manifest formation of plasma bubbles shown in Figs. 4(b). Under this circumstance, the use of $n_{fm} = 5 \times 10^{19} cm^{-3}$ gives P_{cr} = 0.367 TW with respect to the 1030-nm laser; therefore, the ratio $P_L/P_{cr} \sim 1.63$ ensures the onset of self-focusing effect at P_L = 0.6 TW. In contrast, a 0.6-TW, 800-nm laser pulse cannot be focused when propagating in a gas cell of the same density. Because of the growth of self-modulation instability, the laser pulse breaks up into three major micro pulses as shown in Fig. 4(d). The following longitudinal compression thus enhances the intensity of these micro pulses and ultimately amplifies the amplitudes of the excited plasma wave in Fig. 4(b) from t = 0.87 ps. At the same time, the plasma wave undergoes a transverse wave breaking that results in the electron injection in the third bubble, primarily due to its larger wake front curvature that is inherently favourable of inducing electron injection therein [7].

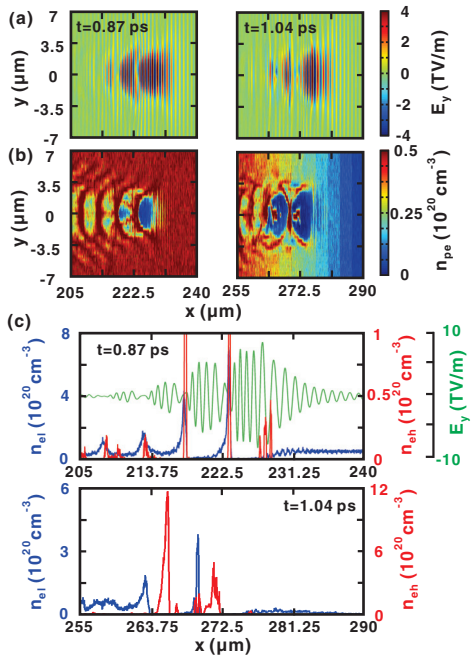

Figure 4: Variations of (a) the E_y field of the incident 1030-nm laser pulse and (b) the density distribution of hydrogen plasma electrons. (c) Comparison of the on-axis densities of the accelerated electron n_{eh} and the plasma electrons n_{el}. The peak density $n_{fm} = 5 \times 10^{19}\text{cm}^{-3}$ is assigned.

ISBN: 978-3-95450-184-7 doi:10.18429/JACoW-IPAC2018-THPML018

EFFECT OF THE GAS CELL LENGTH

Results shown in Fig. 4(b) reveal that, although the first two plasma bubbles have been excited with high amplitudes in the plateau region, a certain distance of evolution is necessary for the associated electron injection to occur in these plasma bubbles. Therefore, the use of an extended length of the plateau region represents a straightforward approach for obtaining the energetic electrons that can be accelerated by the first plasma bubble having the highest amplitude.

Here, the plateau region of the gas target is increased to 260 μm, while keeping the same rest of parameters used in the previous section. As shown in Fig. 5(a), guided propagation of the micro pulses helps to maintain the intensities of these pulses when they move to the edge of the plateau region at x = 300 μm. Consequently, amplitudes of the excited plasma bubbles can be sustained in the extended plateau region, which enables the injection and acceleration of electrons in the region of the first plasma bubble, as shown in Fig. 5(b) at t = 1.12 ps. When these accelerated electrons move together with the plasma bubbles into the following density-down ramp, however, the rapid variation of the bubble size due to the decreasing plasma density in this region can exert additional manipulations to the properties of output electrons. Comparing the energy spectra shown in Fig. 5(d), it can be observed that the drop of maximum energy of the electron from ~ 32 MeV at t = 1.12 ps to ~ 27 MeV at t = 1.24 ps, which can be explained by the phase changes experienced by these energetic electrons when they propagate through the density-down ramp. Consequently, these energetic electrons (> 1 MeV) are produced with a relatively low emittance $\epsilon_{N,y}$ ~ 3.5 π-mm-mrad, with a total charge Q ~ 0.32 nC at the target output.

CONCLUSION

A PIC model was developed to simulate the scheme in which a sub-TW laser pulse is an incident into a thin, high-density gas target having a flat-top distribution. The plateau region of gas target allows the self-focusing and the self-modulation of the laser pulse to develop in a nearly constant plasma condition that is advantageous of producing well-established plasma bubbles to accelerate electrons. In addition to using the 800-nm laser pulses, 1030-nm laser pulses are assigned in simulations to understand their efficacy of driving the sub-TW LWFA. Results show that a successful LWFA process can be realized.

The density $n_{fm} = 5 \times 10^{19} cm^{-3}$ in the plateau region can provide $P_L/P_{cr} \geq 1.63$ to the introduced 0.6-TW, 1030-nm laser pulse; in this way, results show that the effective self-focusing and self-modulation happened on the laser pulse finally result in the excitation of well-established plasma bubbles in the plateau region. By extending the length of the plateau region, effective LWFA process driven by a 0.6-TW, 1030-nm laser pulse can happen in the first plasma bubble, from which accelerated electrons can be acquired with a maximum energy ~ 27 MeV and a total charge Q ~ 0.32 nC.

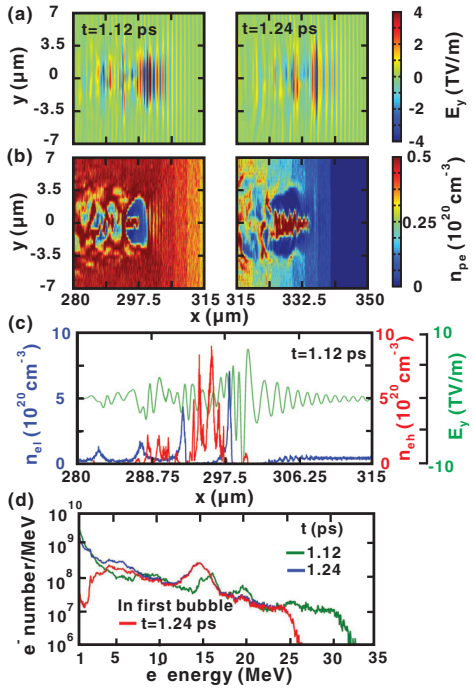

Figure 5: Variations of (a) the E_y field of the incident 1030-nm laser pulse and (b) the density distribution of hydrogen plasma electrons. (c) Comparison of the on-axis densities of the accelerated electron n_{eh} and the plasma electrons n_{el}. (d) The energy spectra about the electrons. The peak density $n_{fm} = 5 \times 10^{19} \mathrm{cm}^{-3}$ and the full length of 340 μm is assigned.

REFERENCES

[1] A. J. Goers, G. A. Hine, L. Feder, B. Miao, F. Salehi, J. K. Wahlstrand, and H. M. Milchberg, Phys. Rev. Lett. **115**, 194802 (2015).

[2] E. Kaksis, G. Almási, J. A. Fülöp, A. Pugzlys, A. Baltuska, and G. Andriukaitis, Opt. Express **24**, 25, 28915 (2016).

[3] G.-Z. Sun, E. Ott, Y. C. Lee, and P. Guzdar, Phys. Fluids **30**, 526 (1987).

[4] E. Caracciolo, M. Kemnitzer, A. Guandalini, F. Pirzio, A. Agnesi, and J. Aus der Au, Opt. Express **22**, 19912 (2014).

[5] M. Siebold, S. Bock, U. Schramm, B. Xu, J.L. Doualan, P. Camy, and R. Moncorgé, Appl. Phys. B **97**, 327 (2009).

[6] C. Nieter and J. R. Cary, J. Comput. Phys. **196**, 448 (2004).

[7] S. V. Bulanov, F. Pegoraro, A. M. Pukhov, and A. S. Sakharov, Phys. Rev.Lett. **78**, 4205 (1997).